



HAL
open science

Unveiling the Nitrogen Chemistry of Titan with the Dragonfly Mass Spectrometer: Experimental Focus on Amines and Amides

Caroline Freissinet, Valentin Moulay, Xiang Li, Cyril Szopa, Arnaud Buch, Antoine Palanca, Victoria da Poian, Alex Abello, David Boulesteix, Sandrine Vinatier, et al.

► To cite this version:

Caroline Freissinet, Valentin Moulay, Xiang Li, Cyril Szopa, Arnaud Buch, et al.. Unveiling the Nitrogen Chemistry of Titan with the Dragonfly Mass Spectrometer: Experimental Focus on Amines and Amides. *ACS Earth and Space Chemistry*, 2024, 8 (9), pp.1832-1846. 10.1021/acsearthspacechem.4c00143 . insu-04671939

HAL Id: insu-04671939

<https://insu.hal.science/insu-04671939v1>

Submitted on 29 Sep 2024

HAL is a multi-disciplinary open access archive for the deposit and dissemination of scientific research documents, whether they are published or not. The documents may come from teaching and research institutions in France or abroad, or from public or private research centers.

L'archive ouverte pluridisciplinaire **HAL**, est destinée au dépôt et à la diffusion de documents scientifiques de niveau recherche, publiés ou non, émanant des établissements d'enseignement et de recherche français ou étrangers, des laboratoires publics ou privés.

Unveiling the Nitrogen Chemistry of Titan with the Dragonfly Mass Spectrometer: Experimental Focus on Amines and Amides

Caroline Freissinet,* Valentin Moulay, Xiang Li, Cyril Szopa, Arnaud Buch, Antoine Palanca, Victoria Da Poian, Alex Abello, David Boulesteix, Sandrine Vinatier, Samuel Teinturier, Jennifer C. Stern, William B. Brinckerhoff, and Melissa G. Trainer



Cite This: <https://doi.org/10.1021/acsearthspacechem.4c00143>



Read Online

ACCESS |



Metrics & More



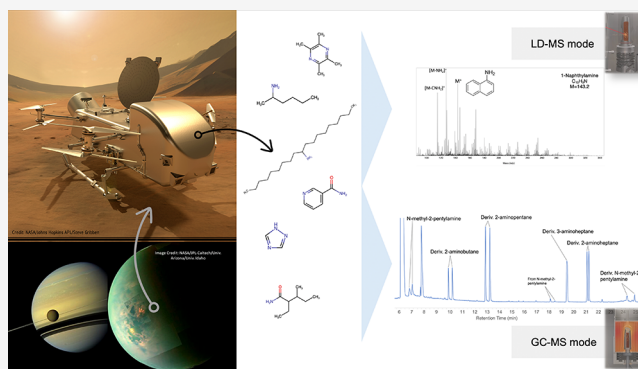
Article Recommendations



Supporting Information

ABSTRACT: The Dragonfly mission payload includes the Dragonfly Mass Spectrometer (DraMS) instrument, which operates in both gas chromatography–mass spectrometry (GCMS) and laser desorption mass spectrometry (LDMS) analysis modes. DraMS will investigate Titan chemistry at geologically diverse locations. Titan uniquely offers direct access to abundant, complex, carbon- and nitrogen-rich chemistry on the surface of a water-ice-dominated ocean world. Amino and amide functional groups, if both present, would be witnesses of redox conditions in the surface environment. An enantiomeric excess in those compounds could help discriminate the chemical or biological origins of these molecules. In this study, we first investigated a wide range of amines and amides (primary, secondary, tertiary, aliphatic, aromatic, branched, and linear moieties) using DraMS-like GCMS protocols, with sample volatilization via both pyrolysis and wet chemistry (derivatization with dimethylformamide dimethyl acetal—DMF-DMA). We determined the general patterns of this derivatization according to the chemical families: dimethylformamidination of the primary amines and amides; methylation, formylation, and dimethoxymethylation of the secondary amines; and lack of derivatization of the secondary amides. The minor coproducts were also identified for each chemical family, to help strict identification of molecules in a Titan GCMS spectrum. The limits of detection and quantification showed that N-species could be detected in the range of tens of fmol to hundreds of pmol. Out of the six chiral amines and amides investigated, five were enantiomerically resolved. We also performed LDMS measurements on a subset of compounds, amines—aliphatic and aromatic—and an amide, and their detection and identification demonstrated the complementarity of LDMS and GCMS modes. Altogether, our results demonstrate the application of DraMS to characterize the expected wide diversity of N-containing compounds of interest at Titan's surface.

KEYWORDS: *DraMS, organic molecules, GCMS, LDMS, Dragonfly, Titan, amines, amides*



INTRODUCTION

Titan's dense atmosphere of nitrogen and methane supports rich organic photochemistry. Energetic particles and ultraviolet (UV) photons dissociate and ionize atmospheric components to produce a suite of carbon–hydrogen–nitrogen ($C_xH_yN_z$) compounds. Experimental gas-phase studies of Titan chemistry indicate that nitriles are the more abundant N-containing molecules.^{1,2} Amino and amide functional groups ($-NR'R''$, and $R-CO-NR'R''$, respectively), if present, may be indicators of redox conditions on the surface of Titan. Amines have been reported as a component of solid Titan analog material, termed tholins, using several measurement techniques (e.g., IR absorption, atmospheric pressure photoionization mass spectrometry, matrix-assisted laser desorption/ionization (MALDI) mass spectrometry, NMR, microcapillary electrophoresis with laser-induced fluorescence, and high-performance liquid

chromatography–Orbitrap mass spectrometry).^{3–11} Yet they have not been extensively reported in papers utilizing pyrolysis–gas chromatography–mass spectrometry (pyr-GCMS) as the primary analysis. Khare et al.¹² reported the detection of four aromatic primary amines (2-amino-pyridine, 2-amino-pyrimidine, aminomethyl-pyridine, and aminomethyl-pyrimidine) using pyr-GCMS of complex Titan analogs. Morisson et al.³ used pyr-GCMS to analyze samples generated from 10% $CH_4/$

Received: May 18, 2024

Revised: July 7, 2024

Accepted: August 1, 2024

90% N₂ gas mixtures, and reported the detection of aminopyridine and tentative detection of ammonia, amino-cyclobutane, 2-propyn-1-amine, and benzylamine. These results suggest a potential bias toward ring-based structures. In Morisson et al.,³ it is discussed that the measurement of linear amines is challenging in GCMS due to their polar nature and adsorption on stainless steel in the GCMS transfer lines. Derivatization approaches are thus used as complementary methods to help detect linear amines. Only a few derivatization experiments have been performed on tholins and none revealed linear amines.^{13,14}

Not all techniques are quantitative. The most quantitative of these is capillary electrophoresis used in Cable et al.,⁴ in which the abundance in Titan analogs ranges from 0.001 to 0.4 wt % for individual aliphatic linear primary amines. It is also noteworthy that despite the use of an extraction technique in the capillary electrophoresis work of Cable et al.,⁴ which was tailored to analyze the soluble and free molecules in the tholins, only a limited number of amines were detected and it was reported that the more volatile amines were detected in a sample kept at ~170 K until the analysis. This observation is relevant to the interpretation of the analysis of tholins with pyr-GCMS in general as most of the samples analyzed with this technique are stored at laboratory ambient temperature, likely resulting in the evaporation of light amines that may have been present in the tholins. It may also indicate that many of the amine groups detected in tholins are associated with large carbon-based molecular structures (both aliphatic and aromatic) that are difficult to extract as intact species for analysis.

Thus, it is not apparent whether the differences between amine detections reported across the literature are a result of the analysis approach, the composition of the sample, the sample handling/storage, or (likely) all three. The pyr-GCMS analysis presented by Morisson et al.³ utilized samples that were of similar provenance to those studied in Gautier et al.,¹ in which amine signatures in IR spectroscopy were reported to be most prevalent in the analog samples made with the lowest CH₄ gas mixture, i.e., 2% CH₄/98% N₂. Interestingly, in the supporting tables from Morisson et al.,³ the 2% CH₄/98% N₂ samples yielded fewer detected compounds overall, yet still include several amines. However, the results are not quantified in the tables, and the relative abundances (or experimental detection limits) of these species are not reported.

The Dragonfly mission, which will explore Titan beginning in the mid-2030s and investigate Titan chemistry at geologically diverse locations,¹⁵ is equipped with the Dragonfly Mass Spectrometer (DraMS) instrument. DraMS is an ion trap mass spectrometer, with a mass range of 15–1950 Da, that can operate in both GCMS and laser desorption mass spectrometry (LDMS) analysis modes.¹⁶ GCMS on DraMS allows a separation and strict identification of volatile compounds extracted from the sample either with heat (pyrolysis up to 600 °C) or chemical reaction (derivatization), using either tetramethylammonium hydroxide (TMAH) or dimethylformamide dimethyl acetal (DMF-DMA) as derivatization reagents. DMF-DMA derivatization not only allows for the extraction and analysis of higher-molecular-weight and more polar compounds than pyrolysis alone but also preserves the chiral center of molecules. LDMS primarily seeks to characterize the refractory and low-volatility organic content by characterizing the mass profiles and identifying specific mass spectral patterns in the organic matter present in the Titan surface samples.

Together, the LDMS and GCMS analyses will enable a substantial compositional survey of organic materials present on various terrains at the Titan surface, with the objectives to understand Titan's complex chemistry and chemical surface processing and possibly identify chemical biosignatures.

Although not an explicit requirement of DraMS, it is of high interest to explore its capabilities for the detection of amines and other N-containing compounds. Except for the analysis of heterocyclic amines,^{17–19} the literature on the derivatization of such chemical families with DMF-DMA is scarce with no published systematic studies. Due to its chemical structure, DMF-DMA carries an electrophilic site on its C as well as a nucleophilic site on its N, which makes it a reactive chemical²⁰ (Figure S1). To achieve the derivatization with DMF-DMA, it is required to heat the sample and the reactant to 145 °C in the laboratory and to slightly higher temperatures (~160 °C) in DraMS due to the melting temperature of the eutectic that releases the reagents. This temperature, although moderate, will favor some chemical reactions in the sample due to the heat alone (soft pyrolysis) and not only to the chemical reaction with DMF-DMA. The combination of soft pyrolysis and derivatization in a DMF-DMA derivatization experiment complicates the analysis of a sample, and a better understanding of each contribution will aid in the interpretation of the data and to work backward to determine the initial composition of organic matter present in the sample. For these reasons, we have tested the DMF-DMA derivatization on a diversity of amines and other N-containing compounds of interest to Titan chemistry. We also tested LDMS analyses on a subset of the compounds investigated in GCMS to evaluate the performance of both techniques to detect and identify the same molecules. We investigated different types of amines (primary, secondary, tertiary, aliphatic, aromatic, linear, and branched), as well as amides. By understanding the GCMS and LDMS signatures of these compounds (e.g., retention times, mass spectra), we can better assess the Dragonfly/DraMS analytical capabilities and anticipate required approaches for the interpretation of Titan nitrogen-chemistry mission data. Limits of detection were also investigated in GCMS, as well as the quantitative differences between under- and derivatized amines, to demonstrate the complementarity of the two methods. The enantiomeric separation of chiral amines was also explored in this study as pure compounds as well as with DMF-DMA derivatization followed by GCMS analysis.

■ MATERIAL AND METHODS

Chemicals and Samples. All chemicals were purchased from Merck and Sigma-Aldrich. Aliphatic primary amines were ethylamine (99%), butylamine (>99.5%), pentylamine (99%), hexylamine (99%), octylamine (99%), nonylamine (99%), decylamine (95%), dodecylamine (>99%), tetradecylamine (95%), hexadecylamine (98%), and octadecylamine (97%). Aromatic primary amines were 1-naphthylamine (99%) and aniline (>99.5%). Branched primary amines were isopropylamine (>99.5%), tert-amylamine (98%), 2-aminobutane (99%), 2-aminopentane (97%), 2-aminoheptane (99%), 3-aminoheptane, 8-aminopentadecane, and 10-aminononadecane (97%). Aliphatic secondary amines were *N*-methylpropylamine (96%), *N*-isopropylmethylamine (98%), *N*-ethyl-*N*-propylamine, and *N*-methyl-2-pentanamine. Aromatic secondary amine was 1,2,3-triazole (98%). Tertiary amines were 4-methylpyridine, 1-propyl-1*H*-1,2,4-triazol-3-amine, *N*-methylpyrrole (99%), 2,3,5,6-tetramethylpyrazine (98%), hexamethylenetetramine

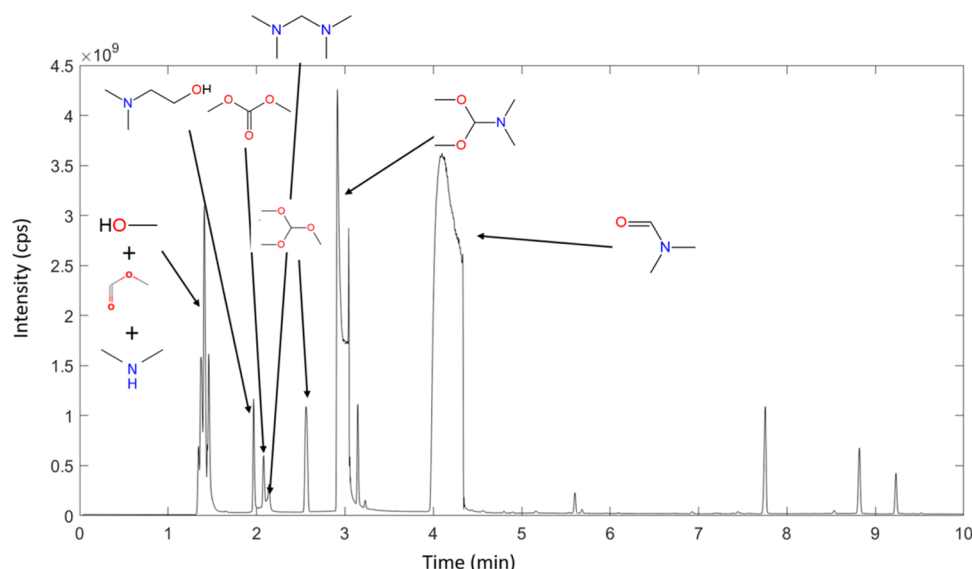


Figure 1. Chromatogram of heated DMF-DMA (derivatization blank, 145 °C, 3 min). GC program: 40 to 300 °C (hold at 300 °C) with a 10 °C·min⁻¹ ramp. Injection of 0.2 μL, split 25. Major compounds are identified in the figure.

(HMT), and triethylamine. Amides were nicotinamide, acetamide (99%), butyramide (98%), *N*-methylacetamide (99%), *N*-ethylacetamide (99%), and 2-ethyl-3-methylpentamide (>96%).

Among those, the chemicals holding a chiral center were 2-aminobutane, 2-aminopentane, 2-aminoheptane, 3-aminoheptane, *N*-methyl-2-pentanamine, and 2-ethyl-3-methylpentamide. All compounds are represented in [Supporting Table S1](#). Given the operating laboratory requirement to perform analysis with the sample placed under vacuum in the system setup, LDMS analyses focused exclusively on nonvolatile samples. Therefore, a selection of samples consisting of tetradecylamine, hexadecylamine, octadecylamine, 1-naphthylamine, and butyramide were studied by LDMS.

GCMS Instrumentation and Methods. Most of the experiments were performed on a Thermo Fisher Scientific Trace 1300 gas chromatograph coupled to a Thermo Fisher Scientific ISQ II quadrupole mass spectrometer. Electronic ionization at 70 eV was used as the source. The MS range was from *m/z* 5 to *m/z* 535. The GC was equipped with a split/splitless injector, and its temperature was set to 250 °C. Carrier gas was helium (as on DraMS) (Air Liquide, purity >99.999%) flowing at a 1 mL·min⁻¹ rate throughout the column. An RTX-20 chromatographic column (Restek, 30 m in length × 0.25 mm ID × 0.25 μm phase thickness) was used. The temperature program was set within the expected DraMS operating limits: initial oven temperature 40 °C, heated to 280 °C with a 10 °C·min⁻¹ ramp, and held for 15 min at the highest temperature. For chiral analyses, a CP-Chirasil-Dex (Agilent –25 m in length × 0.25 mm ID × 0.25 μm phase thickness) was used. In this study, the oven was set to 40 °C and ramped at a rate of 5 °C·min⁻¹ up to 190 °C. The maximum temperature was held for 15 min.

It is worth noting that the two columns present on the DraMS are RTX-5 and Chirasil-Dex. The performances of the RTX-20 and RTX-5 columns with identical dimensions have been shown to be very similar under DraMS-like analytical conditions.¹⁴ Thus, the results obtained with the RTX-20 used for this study can be considered representative of those of the RTX-5 used on DraMS-GC. For Chirasil-Dex, a deeper

exploration of the DraMS columns demonstrated that the actual phase thickness of the stationary phase of the column onboard DraMS may differ from the one used in the laboratory for this investigation and may lead to instrumental variability between both, slightly impacting the direct comparison between laboratory and DraMS measurements.

Qualitative Studies. For all qualitative studies, the amount of the initial compound or derivatized compounds was not strictly maintained. For pyrolysis, about 0.2 μL of each pure compound were injected in the GCMS (the injector was set to 250 °C) with a split ratio of 50:1. For derivatization, see the [Derivatization Procedures](#) Section.

Derivatization Procedures. Derivatization with DMF-DMA (Merck, >99% purity) was performed as follows: 20 μL of DMF-DMA were added to the samples (samples are either liquid or solid form), in a 2 mL glass vial. Qualitative studies did not require any quantification of the sample; a few microliters of the pure liquid sample were typically used, or the minimum visible amount of samples in solid form was used. The vial was then heated up to 145 °C for 3 min²¹ in a block heater. 0.1 or 0.2 μL of the reacted solution was injected into the GCMS with a microsyringe, with a split ratio of 50:1.

For derivatization of racemic mixtures of amines, an equivolumetric solution of each of the five racemic compounds was made, and 1 μL was derivatized with 5 μL of DMF-DMA. For derivatization of the racemic amide, an equivolumetric solution of both enantiomers was made in DMF (10⁻² M of each enantiomer, in DMF). 10 μL of the mixture was derivatized with 20 μL of DMF-DMA. 0.2 μL was injected into the GCMS with a microsyringe, with a split ratio of 50:1.

Blank derivatization samples consisted of DMF-DMA heated by itself in a 2 mL glass vial to 145 °C for 3 min to identify and subtract the byproducts generated by the heat treatment only.

Quantitative Studies. For quantitative studies (limits of detection—LOD, limits of quantification—LOQ), the concentration range of the standard molecules was 1.6 × 10⁻⁵ to 10⁻² mol·L⁻¹, diluted in DMF. Methyl laurate (>98%) was used as an internal standard. Methyl laurate was prepared as 10⁻² M in ethyl acetate (purity 99.8%). Each solute was studied derivatized and underivatized in the same range of

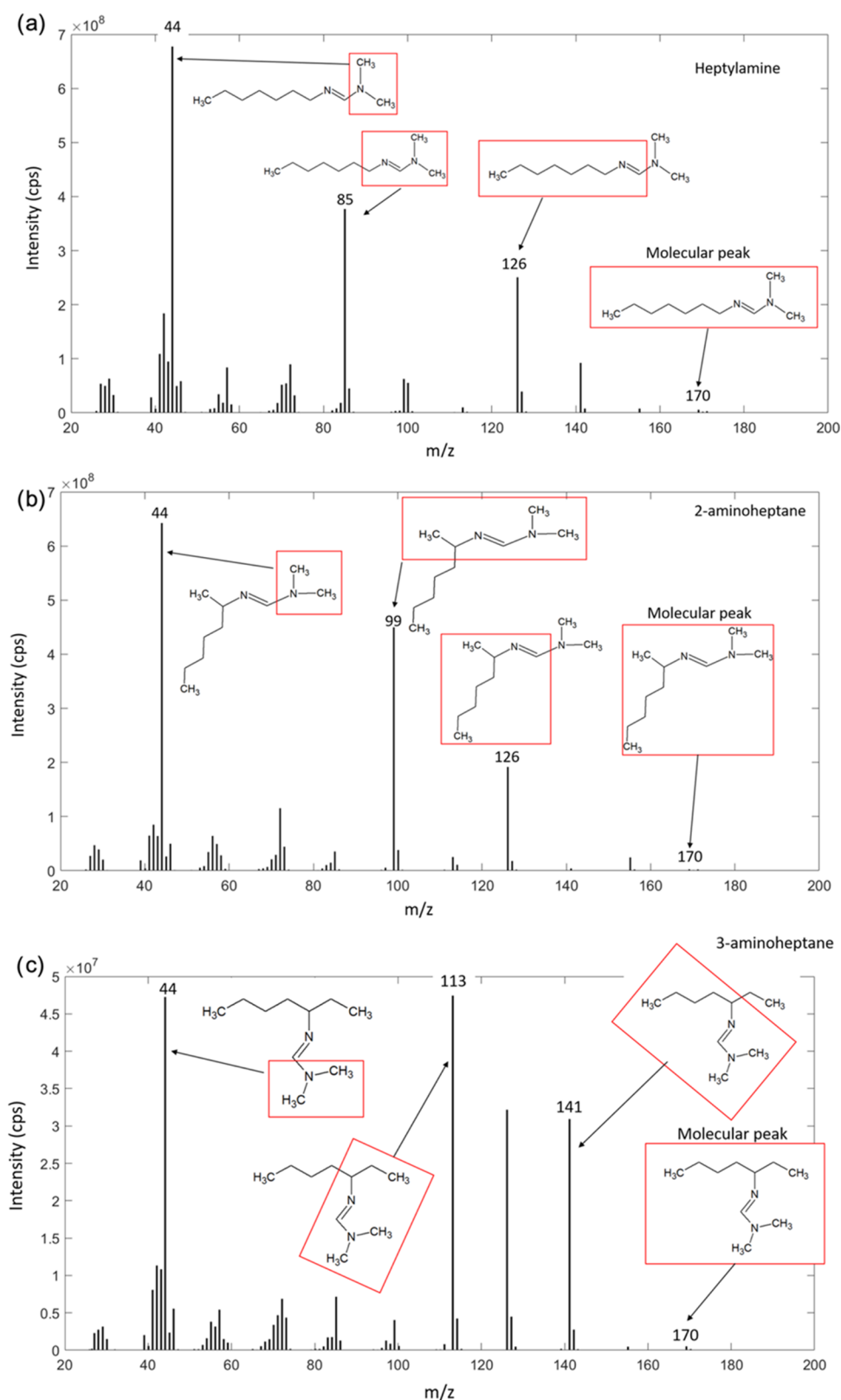


Figure 2. Recognizable mass spectra from a DMF-DMA-derivatized linear aliphatic amine heptylamine (=1-aminoheptane) (a) and branched aliphatic amines 2-aminoheptane (b) and 3-aminoheptane (c), with their ion interpretations.

concentrations, for comparison. 10 μL of underivatized solutions were used, in which 1 μL of internal standard was added. 0.5 μL of it was injected in the GCMS with a split ratio of 1:15. For derivatized solutions, 5 μL of the standard

solutions were mixed with 5 μL DMF-DMA (in molar excess). The reaction occurred at 145 $^{\circ}\text{C}$ for 3 min. After derivatization, 1 μL of the internal standard was added. 0.5 μL of the solution was injected in the GCMS with a split ratio

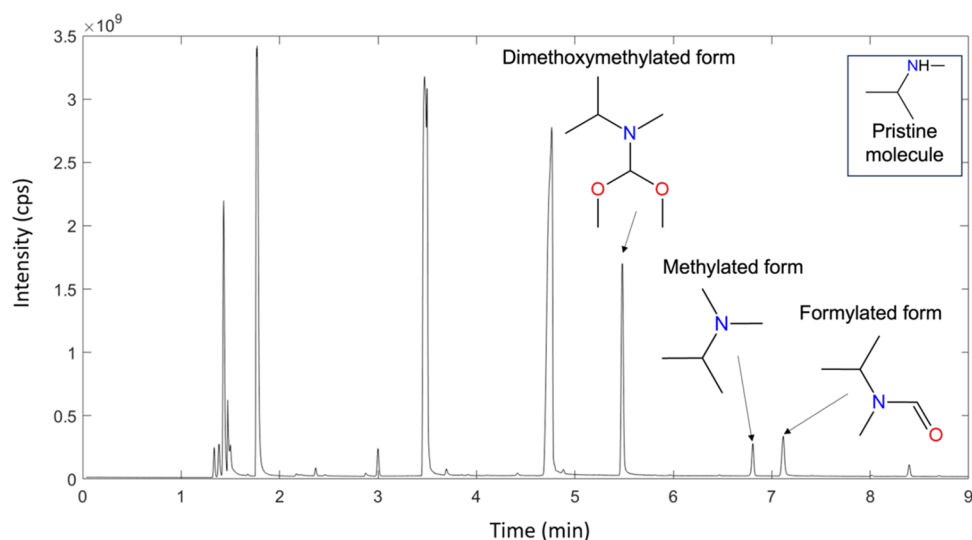


Figure 3. (Top) Chromatogram of *N*-isopropylmethylamine derivatized with DMF-DMA. Three derivatized forms were observed as well as the underivatized form. The other peaks are DMF-DMA byproducts (Figure 1). GC temperature program: 30 to 300 °C with a 10 °C·min⁻¹ ramp, injection 0.1 μL, split ratio 50:1, column RTX-20.

of 1:15. Each experiment was repeated 3 times, and the errors correspond to their standard deviation. The area of the peak of interest (total ion chromatogram, TIC mode) was plotted relative to the area of the peak of the internal standard for normalization.

LDMS Instrumentation and Methods. LDMS prioritizes qualitative studies over quantitative studies, primarily because of the variations arising from the laser desorption process and sample surface morphology. Powdered samples of the studied chemicals were prepared by first dissolving them in dichloromethane, and the solution was then drop-cast onto a highly polished ground stainless steel LDMS target plate. Solvent was used for better adherence of samples to the commercial sample plate and to ensure a more uniform sample surface. Sample plates were loaded into a Bruker Autoflex Speed matrix-assisted laser desorption/ionization (MALDI) time-of-flight (TOF)–mass spectrometer, capable of tandem mass spectrometry (e.g., MS/MS). This instrument is equipped with a pulsed 355 nm laser, up to 1 kHz repetition rate, and a focal diameter of 100 μm. The instrument has a mass resolution as high as 26,000 ($m/\Delta m$ full width at half-maximum), while the maximum registered mass can reach >500,000 u/e. In this investigation, we used the simplest functional capabilities of the instrument to record the mass spectra of the pure chemicals without using any additional matrix in both positive and negative ion modes. MS/MS scans were used to examine the structure of selected compounds through isolation of a parent molecule, fragmentation by collision-induced dissociation (CID), and subsequent mass analysis of the fragment species.

RESULTS

GCMS Analyses. DMF-DMA Alone. Because DMF-DMA contains a nitrogen atom, several of its byproducts are nitrogen-bearing compounds that could interfere with compounds originating from Titan's samples. A typical chromatogram of heated DMF-DMA is presented in Figure 1.

The presence of DMF indicates that a retro-acetalization occurred and converted part of the DMF-DMA into DMF. A coproduct of this reaction is methanol,²² which was also detected. DMF-DMA also dissociated in dimethylamine and

methylformate, observed in Figure 1 at around 1.4 min. Some N-bearing compounds are formed, which would challenge their detection from a Titan sample using DMF-DMA derivatization. All compounds from this blank were considered as analytical background in the sample analyses.

Linear, Branched, and Aromatic Primary Amines. DMF-DMA derivatization of linear ($C_nH_{2n-1}NH_2$) and branched primary amines was close to total (i.e., no underivatized amine detected) and led to a single major derivatized form. The molecule had a dimethylformamidinium group replacing the amine functional group (Figure S1). Aromatic primary amines followed the same reaction; however, the reaction was not total, and minor underivatized forms were detected. As an example, underivatized aniline was observed, about 10 times less abundant than derivatized aniline (ratio of peaks' respective areas).

The fragmentation patterns in the MS for a derivatized linear aliphatic amine and a derivatized branched aliphatic amine are distinguishable (Figure 2). The linear amine undergoes a β -scission, forming a m/z 85 ion ($C_4H_9N_2^+$), while a branched amine with a methyl group on the α -C forms a m/z 99 ion ($C_5H_{11}N_2^+$), and a branched amine with a methyl group on the β -C results in a m/z 113 fragment ($C_6H_{13}N_2^+$). The same trend is followed for other isomers: derivatized 8-amino-pentadecane formed a m/z 183 main ion, and 10-amino-nonadecane formed a m/z 211 fragment. The *tert*-amylamine, having two methyl groups on the α -C, produced a m/z 113 fragment. In most cases, the molecular peak corresponds to $M_{\text{underiv}} + 55$ and is faint, except for small molecules (e.g., isopropylamine).

No methylation or dimethylation was observed on primary amines even though they were considered as potential products.

Minor byproducts were detected: aldehyde counterparts of the linear aliphatic amines and ketone counterparts of the branched aliphatic amines, where an O atom substitutes for the amine functional group. In the absence of DMF-DMA, those aldehydes and ketones were not detected. The pyrolysis alone did not allow this reaction to occur.

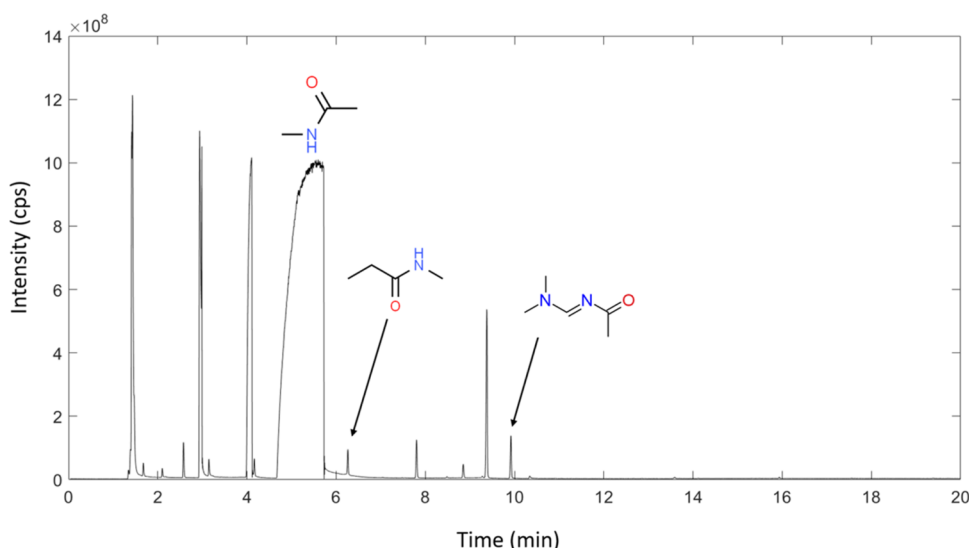


Figure 4. Chromatogram of *N*-methylacetamide (secondary amide) derivatized with DMF-DMA. The derivatized form (RT: 9.9 min) is minor compared to the under-derivatized form (RT: 5 min). The amide indented by one carbon is also observed (RT: 6.2 min).

An exception was the presence of 8-pentacanone in the pyrolysis of 8-aminopentadecane. However, because of the presence of 8-pentacanone and 8-pentadecanol in direct injection of 8-aminopentadecane, it is expected that those two compounds are contaminated from the sample itself.

The linear aliphatic primary amines also led to the formation of the dimethylformamidinium forms of $C_{(n-1)}$ and $C_{(n-2)}$ amines. For example, the decylamine led to the derivatized octylamine and nonylamine, although their signals are 2 orders of magnitude lower than the derivatized decylamine.

Small linear amines (ethylamine, butylamine, pentylamine), branched amines (up to 2-aminopentane) and aromatic amine (aniline) also undergo some dimerization, likely due to the high temperature of the derivatization reaction.

Finally, for linear aliphatic primary amines, nitriles with the same carbon chain length as the initial amine were detected. A pyrolysis-only (without DMF-DMA) analysis performed on the same samples also showed the nitrile, demonstrating that the heat-only case allowed the reaction.²³

We were able to detect up to C_{19} amine 10-amino-nonadecane. The high signal from the derivatized C_{19} amine, coupled to the reasonable retention time (~ 21 min) and column elution temperature (~ 250 °C) under DraMS conditions, hints at the C_{19} amine not being the heaviest linear amine identifiable with DraMS. Unfortunately, higher-molecular-weight amines were not available to purchase from our suppliers such as Merck/Aldrich.

Linear and Aromatic Secondary Amines. Without the two hydrogen atoms present in the primary amines, secondary amines were not expected to undergo dimethylformamidination. Indeed, derivatization of those compounds with DMF-DMA produced three distinct derivatized forms of amines: methylated, formylated, and dimethoxymethylated.

The ratio between the three forms varies from molecule to molecule and did not reveal a specific derivatization pattern. However, methylation was the less abundant derivatized form among the four aliphatic secondary amines, yet the most abundant after derivatization of the aromatic secondary amine. The dimethoxymethylated form was the most abundant form for three aliphatic amines, but the formylated form was the most abundant form for the fourth one.

In addition, some pure (underivatized) amine was still present after derivatization, attesting to different thermodynamic or kinetic effects compared to those for the primary amines (Figure 3).

Tertiary Amines. To evaluate their detection in GCMS, tertiary aliphatic amines were also tested, even though their absence of any hydrogen atom bonded to the nitrogen atom would imply they were not susceptible to derivatization. As expected, no specific reaction with DMF-DMA was observed on the tertiary amine of either of the six molecules tested: aromatics 4-methylpyridine, 1-propyl-1*H*-1,2,4-triazol-3-amine, *N*-methylpyrrole (99%), 2,3,5,6-tetramethylpyrazine (98%), and aliphatic HMT and triethylamine. They were detected as underivatized molecules. 1-Propyl-1*H*-1,2,4-triazol-3-amine also holds a primary amine group, and this molecule is detected as both underivatized and dimethylformamidinated on the primary amine at a lower abundance (~ 5 times less abundant). All six tertiary amines are seen in their underivatized forms on the chromatograms.

Amides. Primary amides were derivatized to form the dimethylformamidinated configuration. Because of the electronic distribution due to the presence of O, primary amides also led to the associated methyl alkanoate, although in a more minor abundance. Some, but not all, of the derivatized amides also generated the dimethylated form. After derivatization, underivatized primary amide was observed at a minor level and for butyramide only, suggesting a near-complete reaction with DMF-DMA.

For secondary amides, the *N*-alkyl group was replaced with an *N*-dimethylformamidinium group to form the dimethylformamidinium derivative. In addition, the amide indented by one carbon was also observed (e.g., *N*-ethylpropanamide is observed after derivatization of *N*-ethylacetamide). After derivatization, the under-derivatized amide is present as the major compound in the runs (Figure 4).

Quantitative Investigations. Quantitative analyses and comparison between derivatized and underivatized amines and amides were performed on pentanamine, decylamine, *N*-ethyl-*N*-propylamine, aniline, and butyramide. For derivatization, DMF-DMA was in molar excess compared to amines, and

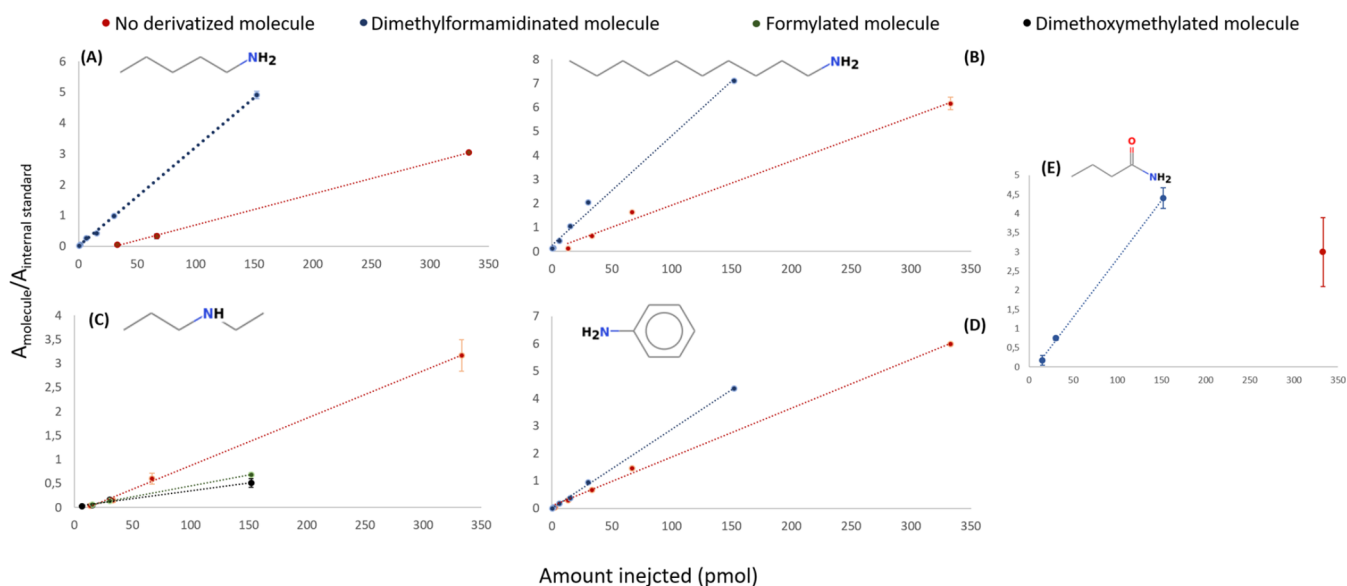


Figure 5. Calibration curves for (A) pentylamine, (B) decylamine, (C) *N*-ethyl-*N*-propylamine, (D) aniline, and (E) butyramide. The area of the GC peak was ratioed to the area of the internal standard.

we did not detect underivatized amines/amides in the chromatograms.

As expected, retention times of the derivatized form, which is heavier, are higher than those of the underivatized forms (Table S2). Pure amine led to peak tailing, while the same amount of derivatized amine displayed a Gaussian-shaped peak (Figure S3). The tailing of the free amines is due to the polarity of the amine functional group. The tailing is suppressed when the amine functional group is derivatized because the polarity is significantly decreased. It translated into different tailing and asymmetry factors between underivatized and derivatized peaks. The tailing factor is computed as $(a + b)/2a$, and the asymmetry factor as b/a , with a and b being the first and last half-width parameters, respectively, at 15% of peak height. As an example, for pure decylamine at 1×10^{-3} mol·L⁻¹ (in DMF), the tailing factor was 2 and the asymmetry factor was 3. The same amount of derivatized decylamine led to a chromatographic peak with both a tailing factor and asymmetry factor of 1.

The GCMS signal was higher for derivatized primary amines and the amide than that for underivatized forms (Figure 5). The DMF-DMA derivatization thus decreased the detection limit of primary amines and amides. The underivatized amide was detected only at the highest concentration. Secondary amines, leading to three derivatized forms, did not display this pattern, and the underivatized secondary amine led to a higher signal than the derivatized ones (Figure 5C).

In the concentration range 1.6×10^{-5} – 10^{-2} mol·L⁻¹ (corresponding to 0.53 pmol to 333 pmol in the GCMS for underivatized compounds, and 0.27 pmol to 167 pmol in the GCMS for derivatized compounds), the strong linearity of the response determined by the squared correlation coefficient values ($R^2 > 0.98$ for each compound, except for the dimethoxymethylated form of the secondary amine) enabled us to investigate the theoretical limits of detection and limits of quantification from our experimental measurements, both for derivatized and underivatized molecules (Table 1). The detection limit X_{LOD} and quantification limit X_{LOQ} were determined as functions of the analyte concentration, yielding a signal value, respectively, $Y_{LOD} = y_b + 6\sigma_b$ and $Y_{LOQ} = y_b +$

$20\sigma_b$, where y_b is the blank average signal generated from 10 blank responses (background signal on the chromatograms used for quantification) and σ_b its standard deviation. The detection and the quantification limits were computed as $X_{LOD} = 6\sigma_b/S$ and $X_{LOQ} = 20\sigma_b/S$, respectively, where S is the slope of the calibration line.

X_{LOD} and X_{LOQ} for underivatized molecules were below the pmol level (initial solution concentration in the μ M level), while it could be in the tens of fmol level for derivatized molecules.

Enantiomeric Separation. Enantiomeric separation of three primary amines (2-aminobutane, 2-aminopentane, and 2-aminoheptane), one secondary amine (*N*-methyl-2-pentanamine), and a primary amide (2-ethyl-3-methylpentamide), derivatized with DMF-DMA and underivatized, was investigated on a Chirasil-Dex GC column. The resolution of the peaks was plotted as $R_s = (t_r^b - t_r^a)/(\omega_a + \omega_b)$, where t_r^a and t_r^b are the retention times of the two peaks and ω_a and ω_b their width at half-height. R_s values higher than 1 correspond to a baseline separation of the two enantiomers and allow calculation of the enantiomeric ratio.

The Chirasil-Dex column did not allow for a satisfactory elution of underivatized primary amines. The excessive tailing caused by the polarity of the molecule on the nonpolar stationary phase thus prevented enantiomeric separation. The DMF-DMA derivatized primary amines, however, led to less polar molecules, resulting in more Gaussian-like peaks, and allowed separation of the three enantiomeric pairs of 2-aminobutane, 2-aminopentane, and 2-amineheptane with a resolution >1 for each (Figure 6b). In contrast, the underivatized chiral primary amide 2-ethyl-3-methylpentamide and the secondary amine *N*-methyl-2-pentanamine both allowed enantiomeric separation on Chirasil-Dex without derivatization (Figure 6c,d). This enantiomeric separation is partial for the amide, and derivatization worsened the resolution of its two enantiomers (Figure 6d). Changes in GC parameters could enhance the enantiomeric separation; however, this was out of the scope of this investigation. For *N*-methyl-2-pentanamine, the derivatized form led to the pair of the formylated form of the derivatization, but also to a residual

Table 1. Limits of Detection and Quantification, X_{LOD} and X_{LOQ} for Both Underivatized and Derivatized forms of Primary Amines, Secondary Amines, and Amide^{a,b}

amines	pure/underivatized				derivatized			
	X_{LOD} pmol	X_{LOD} mol·L ⁻¹	X_{LOQ} pmol	X_{LOQ} mol·L ⁻¹	X_{LOD} pmol	X_{LOD} mol·L ⁻¹	X_{LOQ} pmol	X_{LOQ} mol·L ⁻¹
pentylamine	0.06	1.8×10^{-6}	0.20	6.0×10^{-6}	0.02	1.2×10^{-6}	0.06	3.6×10^{-6}
decylamine	0.19	5.7×10^{-6}	0.65	2.0×10^{-5}	0.04	2.4×10^{-6}	0.14	8.4×10^{-6}
N-ethyl-N-propylamine	0.14	4.2×10^{-6}	0.47	1.4×10^{-5}	dimethoxy 0.27 formyl 0.19	dim. 1.6×10^{-5} form. 1.1×10^{-5}	dimethoxy 0.89 formyl 0.64	dim. 5.3×10^{-5} form. 3.8×10^{-5}
aniline	0.11	3.3×10^{-6}	0.38	1.4×10^{-5}	0.01	6.0×10^{-7}	0.04	2.4×10^{-6}
butyramide	ND	ND	ND	ND	0.22	1.3×10^{-5}	0.74	4.4×10^{-5}

^a X_{LOD} and X_{LOQ} are presented in pmol detected as well as concentration of initial solution. ^bND: not determined.

pair of underivatized form, at about twice the abundance of the formulated form.

LDMS Analyses. Figure 7 shows the mass spectral results obtained with LDMS for relatively large linear amines, in solid phase; specifically tetradecylamine (C₁₄H₃₁N), hexadecylamine (C₁₆H₃₃N), and octadecylamine (C₁₈H₃₉N). In the positive mode of all three spectra, the protonated parent ion ([M + H]⁺) of the amines was detected, although it did not represent the most prominent peak. Across all three cases, the peaks corresponding to [M + H + 51]⁺ and a mass of 208 u exhibited the highest intensity in the spectra. In contrast, the negative mode spectra lack observable parent ions, with the most dominant peaks identified as [M - H + 44]⁻ and a mass of 121 units across all spectra.

In addition to the linear amines, we conducted measurements on an aromatic amine, 1-naphthylamine, and an amide, butyramide, for comparison. The mass spectra in positive mode for these species are shown in Figure 8. Notably, both spectra showed the presence of parent ions (without protonation). In the spectrum of 1-naphthylamine, peaks at lower masses were identified as the fragments derived from the parent ion. However, in the butyramide spectrum, the presence of the *m/z* 51 adduct was once again observed. Negative mode spectra are not shown due to the lack of detection of parent or related peaks in the spectra.

DISCUSSION

Primary amines (-NH₂), secondary amines (-NHR), primary amides (-CONH₂), and secondary amides (-CONHR) hold a polar functional group and thus an inclination to form hydrogen bonds with the matrix or with the stationary phase of the GC column. Table 2 provides a summary of the dominant DMF-DMA reactions and products for all of the chemical classes studied.

Although amines are separated and identified easily on a general RTX-20 midpolar stationary phase, they display a small tailing which expands the peak laterally and thus increases its detection limit. On the Chirasil-Dex stationary phase (with specific presence of cyclodextrins for enantiomeric separation), an underivatized primary amine is not easily analyzable (Figure 6). When derivatized, the primary amine will form a major product, where a dimethylformamidinium group (-N=CH-N-(CH₃)₂) replaces the amino group (-NH₂) (Table 2). The compound is heavier (increase of mass: 55 u) and thus elutes at a later retention time on the column (Table S2). However, the compound is less polar, and the peak shape becomes more Gaussian (tailing and asymmetry factors of 1 for the example of decylamine), which increases the sensitivity when the compound is close to the LOD. Both underivatized and derivatized primary amines are detectable with carbon chain lengths at least up to C₁₉ on the RTX-20 column, and it is expected that the detection can reach higher chain lengths.

It is also interesting to observe that branched primary amine retention times are lower than those of linear primary amines, which would allow branched amines of higher *M_w* to elute within the limited time of analysis dedicated to a DraMS experiment. Adding the fact that the mass spectra of the linear and various isomers of primary amines are easily recognizable (Figure 2), we would be able to identify the structural isomers of amines from a Titan sample with DraMS GCMS. It has also been shown in this study that the limit of detection of derivatized primary amine is improved compared to the one on underivatized primary amine, by a factor of up to 2 orders of

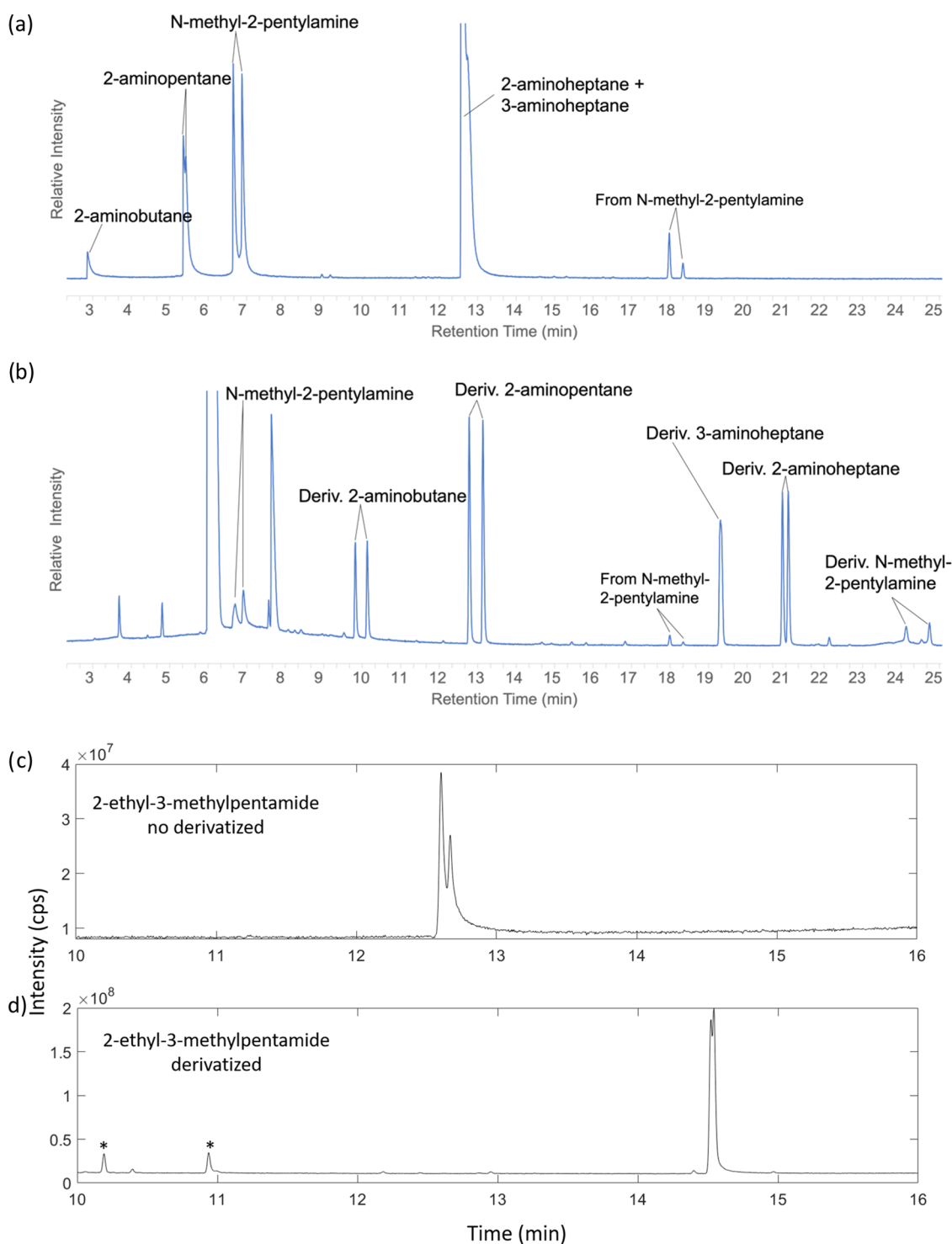


Figure 6. Chromatograms of (a) underivatized and (b) DMF-DMA derivatized mixture of amines: 2-aminobutane, 2-aminopentane, 2-aminoheptane, 3-aminoheptane, and *N*-methyl-2-pentylamine, separated on a Chirasil-Dex GC column. Chromatograms of (c) underivatized and (d) derivatized amide 2-ethyl-3-methylpentamide, separated on a Chirasil-Dex GC column.

magnitude (Table 1 and Figure 5). Having the same initial quantity of compounds in the derivatized vs nonderivatized experiments, the differences in detection between derivatized and underivatized primary amines/amides may be due to chromatographic parameters: (1) the more Gaussian peak shape of the derivatized compounds (less polar) makes it easier to integrate for area and (2) the ionization cross section of the derivatized molecule is higher than the underivatized one; thus,

ionization is more efficient and leads to a higher signal on the MS.

With the Chirasil-Dex column, we were able to detect the derivatized molecule but also to perform a chiral separation and calculate their enantiomeric ratio (Figure 6). On the contrary, the derivatized amide showed a degraded resolution that made its enantiomeric separation harder compared to the underivatized amide.

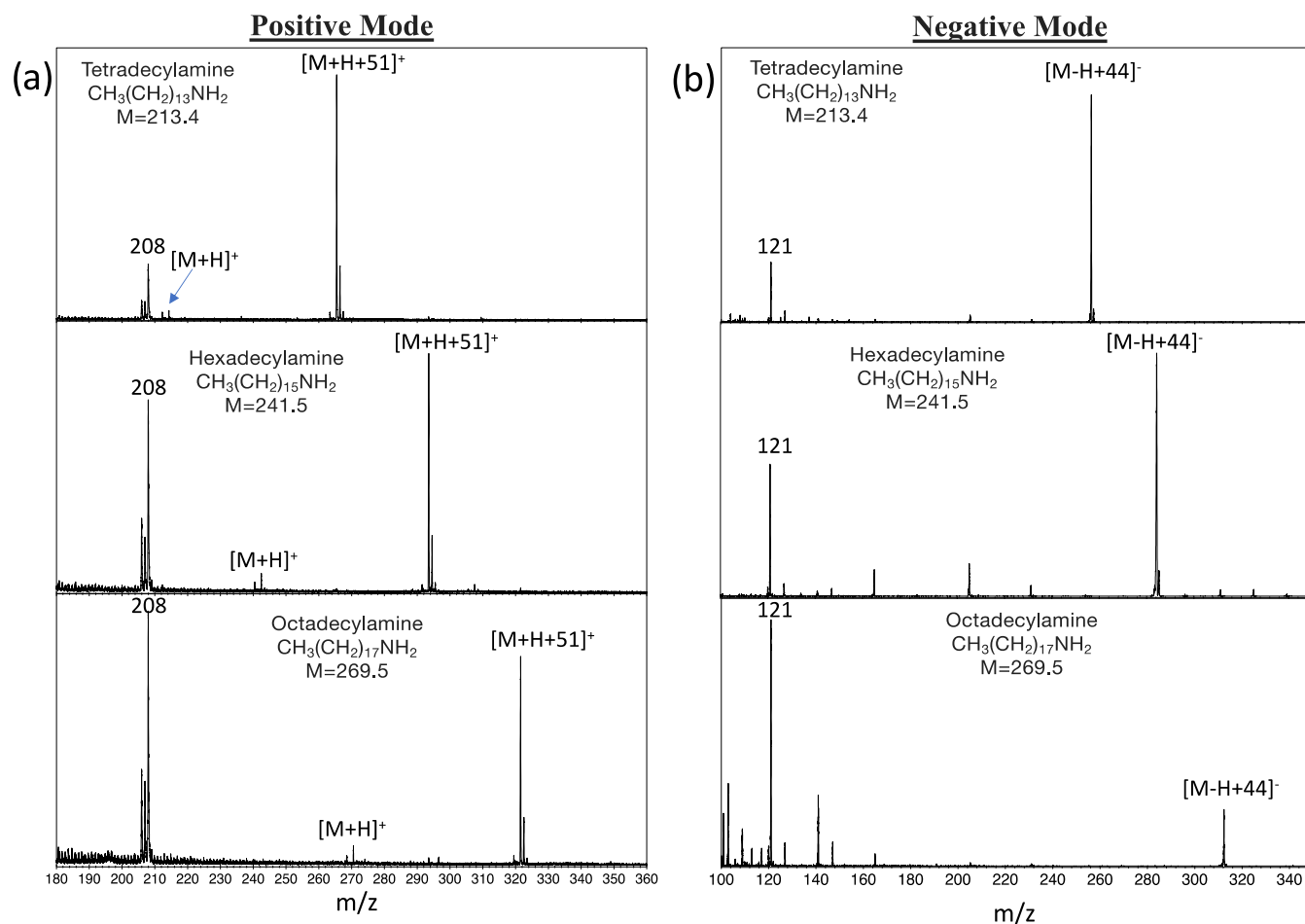


Figure 7. Mass spectra of the linear amines with positive mode (a) and negative mode (b). Protonated parent ions, along with strong adduct peak (adding mass of 51 u) and 208 peak, were observed in the positive mode. Yet only an adduct peak (adding mass 44 u) and m/z 121 peak were evident in the negative mode.

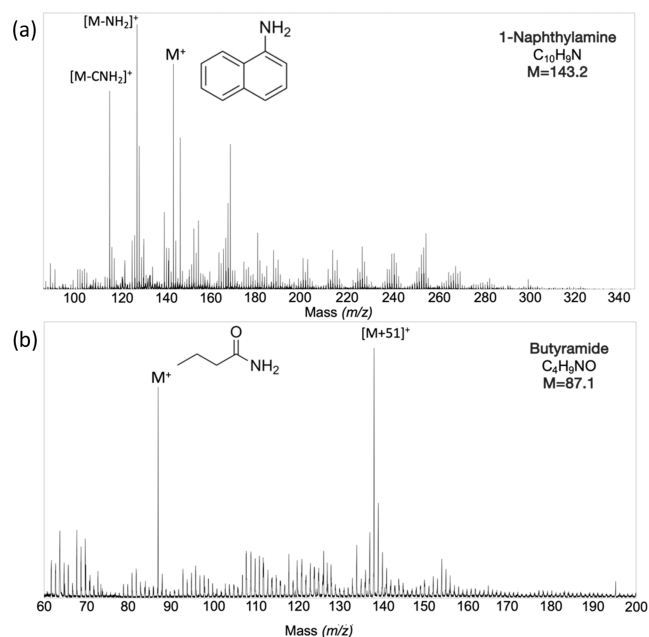


Figure 8. Mass spectra of 1-naphthylamine (a) and butyramide (b) in positive mode. Parent ions were observed in both cases. Fragments presented in the 1-naphthylamine spectrum, and the adduct (adding mass of 51) peak were detected in the butyramide spectrum.

Secondary amines can unexpectedly form three derivatives under DMF-DMA reaction: a methylated, a dimethoxymethylated, and a formylated one (Figures 3 and S2), in no predictable abundance. We were able to identify the formylation and dimethoxymethylation thanks to a former publication,²⁴ as the mass spectra of those did not correspond to existing data in the NIST library. The reactions proposed by Grubb et al.²⁴ imply a retro-acetalization that converts the dimethoxymethylated amine into the formylated amine. Being split into three products and the underivatized form, the limit of detection of each of the derivatized forms is thus higher than the limit of detection of the pure amine, although on the same order of magnitude as the tenth of pmol in this instrumentation (Table 1). Secondary amides mostly do not react with DMF-DMA. However, we could detect the presence of the dimethylformamidinated form as a minor product, which corresponds to the integral substitution of the *N*-alkyl group with a dimethylformamidine group. In that latter case, the information on the length of the carbonated chain of the amide is thus lost.

The dimethylformamidination of the primary aliphatic amines (linear or branched) and the primary aliphatic amides is total when the DMF-DMA is in excess. The derivatization of secondary amines and amides is not total, and the presence of the underivatized form is present on the chromatogram; for secondary amides, the underivatized form is the majoritarian

Table 2. Summary of the Major and Minor DMF-DMA Derivatization Products from the Different Types of Amines and Amides in a GCMS Analysis

molecules (example)	type	main DMF-DMA deriv. product	minor coproducts	remarks
ethylamine (C ₂) to octodecylamine (C ₁₈) isopropylamine	primary aliphatic amine (linear and branched)	dimethylformamidination	aldehydes (linear) ketones (branched)	branched and linear lead to recognizable MS patterns better enantiomeric separation on Chirasil-Dex when derivatized
2-aminobutane			derivatized C _(n-1) and C _(n-2) amine	
2-aminopentane			dimerization on small amines up to C ₅ (heat only—no DMF-DMA required)	
2-aminoheptane			nitriles (heat only—no DMF-DMA required)	
3-aminoheptane				
8-aminopentadecane (C ₁₅) 10-aminononadecane (C ₁₉) tert-amylamine				
aniline 1-naphthylamine	primary aromatic amine	dimethylformamidination	underivatized form dimerization (aniline)	
acetamide	primary aliphatic amide	dimethylformamidination	methyl alkanoate	worst enantiomeric separation on Chirasil-Dex when derivatized (2-ethyl-3-methylpentanamide)
butyramide			underivatized form (butyramide)	hard to identify underivatized at low abundances
2-ethyl-3-methylpentanamide nicotinamide	primary aromatic amide	dimethylformamidination	methyl alkanoate dimethylation underivatized form methylation	
N-methylpropylamine N-isopropylmethylamine N-ethyl-N-propylamine N-methyl-2-pentanamine	secondary aliphatic amine	formylation underivatized form dimethoxymethylation		
1,2,4-triazole	secondary aromatic amine	methylation (96%) dimethoxymethylation formylation	underivatized form	
N-methylacetamide N-ethylacetamide	secondary aliphatic amide	underivatized form	dimethylformamidination C _(n+1) amide	In dimethylformamidination, Integral replacement of the N-alkyl group, the C-chain length is lost

form observed. Different temperatures and durations of derivatization (80 to 300 °C, 30 s to 60 min) were tested, but variation on derivatization conditions on secondary amides did not lead to any improvement of the derivatization yield. This implies a thermodynamic limitation of the reaction on secondary amines. The specific electronic repartition in the amino group in both types of compounds (primary vs secondary) may explain their difference in reactivity. In addition, all types of compounds display additional, although often minor, molecules present in the sample after the derivatization reaction.

Aliphatic linear and branched primary amines substitute for their amine functional group, leading to aldehydes and ketones, respectively. The presence of derivatized C₋₁ and C₋₂ amine demonstrates a decarbonation of the initial amine, followed by derivatization. The heat of the derivatization reaction also led to the formation of nitriles from the initial primary amine and dimerization on small amines. Because of the electronic distribution due to the presence of O, primary amides also led to the associated methyl alkanoate, although in more minor abundance. Some of the derivatized amides, but not all, also generated the dimethylated form. It was expected that the primary amides could lead to a nitrile through dehydration; however, no nitrile was observed. For secondary amides, the

amide indented by one carbon was also observed (e.g., N-ethylpropanamide is observed after derivatization of N-ethylacetamide).

We tested if the aromaticity of the molecule could alter the derivatization, as the aromaticity of the heterocycle weakens the nucleophilic reactivity of the nitrogen as it relocates and flattens the electronic distribution evenly on the atoms of the aromatic ring. While the aromatic core attracts electrons via inductive and mesomeric effects, aliphatic molecules, on the other hand, give electron density to the nitrogen via inductive effect only. A slight difference was observed in the derivatization of aromatic primary amines and amides: although the major derivatized compound was the expected dimethylformamidinated form, we noticed the presence of some under-derivatized aromatic amines and amide. The secondary amines displayed no difference in their derivatization, whether aliphatic or aromatic; both led to the three derivatized forms as well as the underivatized forms.

The mass spectra can be characteristic of the type of molecule; on primary amines, the mass of the fragment resulting from the β-break up depends on the position of the —NH₂ group on the carbon skeleton. On the first carbon (linear), we observe the ion *m/z* 85, while on the second carbon (branched) we observe the ion *m/z* 99 and on the third

carbon, we observe the ion m/z 113. It is expected that a branched amine with the $-NH_2$ group on the fourth carbon would break up in an ion m/z 127 and so on. The ion fragmentation in the mass spectrometer thus gives information about the isomer detected, while the molecular peak is the same.

Because most of the mass spectra generated from derivatization of amines and amides are absent from the NIST spectral database, we thus generated a new “DMF-DMA” database in which we have added all of the new compounds and that will help in identification of DMF-DMA derivatized amines in future experiments and in the analysis of data returned from DraMS-GCMS once on Titan.

In this study, the analysis of volatile and semivolatile substances mainly relied on GCMS because of the vacuum system in the commercial LDMS that evacuates the more volatile amines and amides studied, LDMS is a powerful analytical tool for the examination of nonvolatile samples, typically those with relatively larger molecular masses that are challenging, if not impossible, to detect in GCMS. In this study, LDMS was utilized to analyze linear amines characterized by extended chain lengths, specifically C_{14} , C_{16} , and C_{18} linear amines or compounds with a melting point above room temperature (1-naphthylamine, butyramide). One of the objectives is to evaluate the overlapping range of compounds analyzable in both GCMS and LDMS modes. It is important to note that unlike the commercial instrument, DraMS does not require the samples to be under vacuum for LDMS analysis and thus may allow for the detection of a few of the lower-molecular-weight amines.

In the positive-mode LDMS spectra of linear amines, the detection of protonated parent ions highlights the promising potential of LDMS techniques in identifying key organics. Therefore, its application, such as on the DraMS instrument aboard the Dragonfly mission to Titan, holds great promise for effectively identifying crucial organic compounds on Titan, where organics such as amines are anticipated to be relatively abundant. However, it is important to acknowledge the complexity introduced by potential clusters, adducts, and fragment peaks in the mass spectra, which can raise challenges for data interpretation. For instance, the consistent appearance of a mass increase of 51 u in the adducts of each parent ion contributes to a more prominent signal in the mass spectra. Additionally, a robust peak at m/z 208 persists across all cases. We speculate that the mass increment of 51 u may represent a species with a more stable or reactive structure attached to the parent ions. Efforts were made to assign each peak through utilization of the MS/MS technique, suggesting that the 51 u adduct could be associated with a cyanoacetylene C_3HN adduct ion to the parent compound. Furthermore, m/z 208 likely corresponds to a fragment derived from the $[M + H + 51]^+$ adduct peak, with its enhanced stability against multiphoton excitation (either electronically or structurally) contributing to this distinctive peak. Detailed MS/MS spectra and peak assignments are provided in the Supporting Information (Figures S4 and S5). In negative mode spectra, on the other hand, no parent ion was detected, but prominent adducts of $[M + 43]^-$ have been observed. Given the common tendency in negative mode spectra for the formation of deprotonated species to maintain a negative charge, it is more likely that the $[M + 43]^-$ adduct corresponds to a deprotonated M plus 44 ($[M - H + 44]^-$ as labeled in Figure 7), for the simplest ethyleneamine $CH_2CH_2NH_2$. Overall,

when analyzing linear amines, the positive mode exhibits greater potential for detecting the parent ion. However, in both positive and negative modes, the presence of adducts introduces complexity as well as insights into spectral interpretation.

In the case of chemicals like 1-naphthylamine and butyramide, the parent ions appeared more prominently without protonation and presented as relatively stronger peaks in the spectra compared to the protonated parent ions observed with linear amines. Specific structures such as aromatic functional groups are known to couple well with the UV laser wavelength, resulting in the detection of relatively strong peaks. Note again that in these spectra, there were additional fragment peaks or series of peaks across a wider mass range. For example, some of the weaker peaks exhibited patterns indicative of hydrocarbons, likely originating from clusters formed by laser-desorbed amines.

To Titan. In Morisson et al.,³ tholins were analyzed in pyr-GCMS which led to the detection and identification of many nitrile compounds, but only a few free amines were tentatively reported. It was stated that the measurement of linear amines was challenging in GCMS due to their polar nature and adsorption on stainless steel in the GCMS transfer lines. We have demonstrated that if present in the sample, amines of various sorts (primary, secondary, aromatic, aliphatic, linear, branched) as well as amides (primary, secondary) would be detected in pyrolysis-GCMS, besides other minor coproducts. In addition, when derivatized with DMF-DMA, the free amines transform into less polar forms, and the derivatization product depends on the nature of the amine or amide. The combination of pyrolysis and derivatization in two independent experiments on DraMS would give true confirmation of the presence of those compounds, each leading to different products and thus different (and characterized) retention times on the GCMS, thus increasing the chances of not having overlapping compounds. Derivatization with DMF-DMA will aid in improving the limit of detection of amines and other refractory compounds in complex samples by rendering them less polar. Moreover, DMF-DMA serves to enhance the extraction of bonded molecules from solid samples in a one-pot, one-step experiment.²¹ It also serves to protect the structure and thus avoid recombination during the high-temperature pyrolysis derivatization step.²¹ However, derivatization does not necessarily lead to one unique and identifiable compound. In many cases, a distribution of coproducts is detected in the der-GCMS, several of them with unknown mass spectra in referenced libraries. Nevertheless, the distribution of compounds produces a specific GCMS pattern characteristic of the initial organic composition of the sample. In addition to this challenge and because DMF-DMA itself contains N and creates complex nitrogenated byproducts, the analysis of indigenous N-compounds in a Titan sample is complex and necessitates several laboratory iterations. Lastly, the sample itself could interfere with DMF-DMA, particularly if it contains water or ammonia in high abundance. To overcome this issue, the nominal DMF-DMA derivatization procedure on DraMS will include a sample boil-off to remove the volatile H_2O and NH_3 before the derivatizing reagent is released.

Derivatization with DMF-DMA has been shown to be essential to separate the enantiomers of primary amines on the enantioselective Chiral-Dex GC column. Although few references discuss the importance of chiral amines in biological

systems, some of the main neurotransmitters in many animals and even single-celled organisms (e.g., adrenaline and derivatives) are chiral molecules with an amine functional group.²⁵ The presence of chiral compounds and their enantiomeric purity are key factors in the search for chemical biosignatures in Titan samples. Additional information is needed to be comprehensive on the analysis of nitrogenated compounds and chirality on Titan's sample by DraMS (racemization, low and high mass weight limits). However, this extensive study lessens the concerns of the detection of polar nitrogen-containing compounds with DraMS, as up to at least C₁₉ amines (and up to C₁₈ detected both on the general and on the chiral column in the laboratory) were detected under DraMS-compatible conditions,¹⁴ and down to tens of fmol limits of detection with a laboratory analytical instrument. In GCMS mode, the DraMS instrument detects targeted organic molecules present at 10–100 pmol in the sample. Even when present at low abundances, the LOD for the amines will be comparable in the complex sample to that for the pure compounds when the single ion chromatograms are used to detect and identify minor compounds. The limited detection of amines in tholins reported in the literature is thus likely due to their absence as free amines or to their volatilization during the sample handling prior to analysis. It may also indicate that many of the amine groups detected in tholins, with techniques other than pyr-GCMS, are associated with large carbon-based molecular structures (both aliphatic and aromatics) that are difficult to extract with heat only. The derivatization with DMF-DMA may help in that purpose.

In addition to DMF-DMA, DraMS also carries a thermochemolysis reagent, tetramethylammonium hydroxide (TMAH), and is evaluating the possibility to include trimethylsulfonium hydroxide (TMSH). The thermochemolysis reagents are used to methylate reactive compounds with a labile hydrogen at high temperatures (500–600 °C), a temperature at which macromolecules may fragment into lighter and more volatile compounds, potentially liberating functional groups such as amines. TMAH/TMSH has been shown very efficient in the thermochemolysis, detection, and identification of nucleobases.²⁶ The complementarity of pyrolysis, DMF-DMA derivatization, and TMAH/TMSH thermochemolysis prior to GCMS analyses is a key asset for the strict identification of the complex mixtures that are expected on Titan, particularly toward its nitrogen chemistry.

As observed in the reported LDMS results, the direct mass spectra can be complex, particularly when detecting samples on planetary bodies such as Titan, where an abundance of organic species including various types of amines is expected to be present. Therefore, it becomes crucial to incorporate complementary information not only between positive and negative modes but also across different techniques, such as LDMS and GCMS. The results presented here demonstrate that a range of high-molecular-weight linear amines (C₁₄ to C₁₈), as well as an aromatic amine of low molecular weight (*M_w* 143) but sufficiently high melting point (~50 °C), as well as an amide, butyramide (*M_w* 87, mp ~115 °C), can be detected and identified in both GCMS and LDMS. Specifically, the DraMS instrument aboard the Dragonfly mission targets a mass range of up to 1950 Da for LDMS analysis,¹⁶ capable of detecting very long linear amines up to ~C₁₂₀ if present. Furthermore, the instrument will collect and analyze icy samples²⁷ under low temperatures (<175 K) on Titan. Consequently, LDMS could potentially provide enhanced

capabilities for accessing and analyzing certain volatile substances that might freeze in Titan's environment, which could result in more comprehensive analysis when coupled with GCMS. The integrated approach enhances the accuracy of understanding the analyzed sample by overcoming the challenges associated with individual modes and techniques.

CONCLUSIONS

The design and operation of the DraMS instrument will allow the detection of amines and amides in DraMS-pyrolysis-GCMS, DraMS-derivatization-GCMS, and DraMS-LDMS modes. Derivatization with DMF-DMA of several chemical families and structurally different N-compounds (primary, secondary, tertiary, aliphatic, aromatic, branched, or linear amines and amides) determined their unique pattern, from dimethylformamidination of primary amines and amides, to three derivatized forms of secondary amines, to mostly underivatized secondary amides. Several minor reaction products allow robust identification of the parent molecule. Derivatization with DMF-DMA will also aid in improving the limit of detection of amines and amides on the general GC columns in complex samples by rendering them less polar. The combination of pyrolysis and derivatization helps to strictly identify certain compounds that may coelute. As for chiral compounds, their enantiomers could be better separated (and thus quantified) when derivatized and analyzed on the Chirasil-Dex GC column, apart from the amide, which shows a better enantiomeric resolution underivatized. A subset of molecules was also analyzed in LDMS, and the detection of those in both positive mode and negative mode strengthens the case for a robust inventory of N-compounds on Titan. However, it was also shown that both the chemistry of DMF-DMA derivatization and the interpretation of MS spectra from LDMS, on both amines and amides, are various and complex. As shown, laboratory investigations are thus necessary to better anticipate the understanding of complex data on N-containing compounds that are expected to be obtained with Dragonfly on Titan.

ASSOCIATED CONTENT

Supporting Information

The Supporting Information is available free of charge at <https://pubs.acs.org/doi/10.1021/acsearthspacechem.4c00143>.

List of the compounds investigated in this study, their chemical families and types, and their structures (Table S1); retention time of underivatized and derivatized amines and amides (cf. material and methods for experimental conditions) (Table S2); proposed mechanism of DMF-DMA derivatization on primary amines and secondary amines, chromatograms of pentylamine vs derivatized pentylamine, additional LDMS experiments, MS/MS, and further interpretation (Figures S1–S5 and text) (PDF)

AUTHOR INFORMATION

Corresponding Author

Caroline Freissinet – LATMOS-IPSL/CNRS/UVSQ/Univ. Paris Saclay, 78280 Guyancourt, France; orcid.org/0000-0002-6528-330X; Email: caroline.freissinet@latmos.ipsl.fr

Authors

Valentin Moulay – LATMOS-IPSL/CNRS/UVSQ/Univ.

Paris Saclay, 78280 Guyancourt, France

Xiang Li – NASA Goddard Space Flight Center, Greenbelt, Maryland 20771, United States

Cyril Szopa – LATMOS-IPSL/CNRS/UVSQ/Univ. Paris Saclay, 78280 Guyancourt, France

Arnaud Buch – Laboratoire de Génie des Procédés et Matériaux, CentraleSupélec, 91190 Gif-sur-Yvette, France

Antoine Palanca – LATMOS-IPSL/CNRS/UVSQ/Univ. Paris Saclay, 78280 Guyancourt, France

Victoria Da Poian – NASA Goddard Space Flight Center, Greenbelt, Maryland 20771, United States; Microtel LLC, Greenbelt, Maryland 20771, United States; Earth and Planetary Science Department, Johns Hopkins University, Baltimore, Maryland 21210, United States

Alex Abello – LATMOS-IPSL/CNRS/UVSQ/Univ. Paris Saclay, 78280 Guyancourt, France; orcid.org/0009-0000-6727-6536

David Boulesteix – Laboratoire de Génie des Procédés et Matériaux, CentraleSupélec, 91190 Gif-sur-Yvette, France

Sandrine Vinatier – LESIA, Observatoire de Paris, Université PSL, Sorbonne Université, Université Paris Cité, CNRS, 92195 Meudon, France

Samuel Teinturier – NASA Goddard Space Flight Center, Greenbelt, Maryland 20771, United States; Department of Physics, CUA, Washington, District of Columbia 20064, United States; CRESS II, NASA/GSFC, Greenbelt, Maryland 20771, United States

Jennifer C. Stern – NASA Goddard Space Flight Center, Greenbelt, Maryland 20771, United States

William B. Brinckerhoff – NASA Goddard Space Flight Center, Greenbelt, Maryland 20771, United States

Melissa G. Trainer – NASA Goddard Space Flight Center, Greenbelt, Maryland 20771, United States

Complete contact information is available at:

<https://pubs.acs.org/10.1021/acsearthspacechem.4c00143>

Notes

The authors declare no competing financial interest.

ACKNOWLEDGMENTS

C.F., V.M., C.S., A.B., A.P., A.A., D.B., and S.V. thank the French space agency (CNES) for funding of the GCMS part of this research, within the framework of the Dragonfly APR. S.T. appreciates support through NASA under award number 80GSFC21M0002. The authors also thank the NASA New Frontiers Program and Dragonfly Mission for funding. The Dragonfly Mission is managed by the Johns Hopkins Applied Physics Laboratory under contract to the Planetary Missions Program Office at Marshall Space Flight Center (MSFC) under contract NNN06AA01C.

REFERENCES

- (1) Gautier, T.; Carrasco, N.; Buch, A.; Szopa, C.; Sciamma-O'Brien, E.; Cernogora, G. Nitrile gas chemistry in Titan's atmosphere. *Icarus* **2011**, *213* (2), 625–635.
- (2) Bernard, J. M.; Coll, P.; Coustenis, A.; Raulin, F. Experimental simulation of Titan's atmosphere: Detection of ammonia and ethylene oxide. *Planet. Space Sci.* **2003**, *51* (14–15), 1003–1011.
- (3) Morisson, M.; Szopa, C.; Carrasco, N.; Buch, A.; Gautier, T. Titan's organic aerosols: Molecular composition and structure of

laboratory analogues inferred from pyrolysis gas chromatography mass spectrometry analysis. *Icarus* **2016**, *277*, 442–454.

(4) Cable, M. L.; Horst, S. M.; He, C.; Stockton, A. M.; Mora, M. F.; Tolbert, M. A.; Smith, M. A.; Willis, P. A. Identification of primary amines in Titan tholins using microchip nonaqueous capillary electrophoresis. *Earth Planet. Sci. Lett.* **2014**, *403*, 99–107.

(5) Drenne, S.; Coelho, C.; Anquetil, C.; Szopa, C.; Rahman, A. S.; McMillan, P. F.; Corà, F.; Pickard, C. J.; Quirico, E.; Bonhomme, C.; et al. New insights into the structure and chemistry of Titan's tholins via ¹³C and ¹⁵N solid state nuclear magnetic resonance spectroscopy. *Icarus* **2012**, *221*, 844–853, DOI: [10.1016/j.icarus.2012.03.003](https://doi.org/10.1016/j.icarus.2012.03.003).

(6) Quirico, E.; Montagnac, G.; Lees, V.; McMillan, P. F.; Szopa, C.; Cernogora, G.; Rouzard, J.-N.; Simon, P.; Bernard, J.-M.; Coll, P.; et al. New experimental constraints on the composition and structure of tholins. *Icarus* **2008**, *198*, 218–231, DOI: [10.1016/j.icarus.2008.07.012](https://doi.org/10.1016/j.icarus.2008.07.012).

(7) He, J.; Buch, A.; Carrasco, N.; Szopa, C. Thermal degradation of organics for pyrolysis in space; Titan's atmospheric aerosol case study. *Icarus* **2015**, *248*, 205–212, DOI: [10.1016/j.icarus.2014.10.010](https://doi.org/10.1016/j.icarus.2014.10.010).

(8) Gautier, T.; Carrasco, N.; Mahjoub, A.; Vinatier, S.; Giuliani, A.; Szopa, C.; Anderson, C. M.; Correia, J.-J.; Dumas, P.; Cernogora, G. Mid- and far-infrared absorption spectroscopy of Titan's aerosols analogues. *Icarus* **2012**, *221* (1), 320–327.

(9) Hiroshi, I.; Dale, P. C.; Christopher, P. M.; Seiji, S.; Bakes, E. L. O.; Bishun, N. K.; Takafumi, M.; Richard, N. Z.; Jamie, E. E. Laboratory experiments of Titan tholin formed in cold plasma at various pressures: implications for nitrogen-containing polycyclic aromatic compounds in Titan haze. *Icarus* **2004**, *168*, 344–366, DOI: [10.1016/j.icarus.2003.12.014](https://doi.org/10.1016/j.icarus.2003.12.014).

(10) Gautier, T.; Schmitz-Afonso, I.; Touboul, D.; Szopa, C.; Buch, A.; Carrasco, N. Development of HPLC-Orbitrap method for identification of N-bearing molecules in complex organic material relevant to planetary environments. *Icarus* **2016**, *275*, 259–266, DOI: [10.1016/j.icarus.2016.03.007](https://doi.org/10.1016/j.icarus.2016.03.007).

(11) Carrasco, N.; Tigrine, S.; Gavilan, L.; Nahon, L.; Gudipati, M. S. The evolution of Titan's high-altitude aerosols under ultraviolet irradiation. *Nat. Astron.* **2018**, *2* (6), 489–494.

(12) Khare, B. N.; Sagan, C.; Thompson, W. R.; Arakawa, E. T.; Suits, F.; Callcott, T. A.; Williams, M. W.; Shrader, S.; Ogino, H.; Willingham, T. O.; Nagy, B. The organic aerosols of Titan. *Adv. Space Res.* **1984**, *4* (12), 59–68.

(13) Hörst, S.; Yelle, R. V.; Buch, A.; Carrasco, N.; Cernogora, G.; Dutuit, O.; Quirico, E.; Sciamma-O'Brien, E.; Smith, M. A.; Somogyi, Á.; et al. Formation of Amino Acids and Nucleotide Bases in a Titan Atmosphere Simulation Experiment. *Astrobiology* **2012**, *12* (9), 809–817.

(14) Moulay, V.; Freissinet, C.; Rizk-Bigourd, M.; Buch, A.; Ancelin, M.; Couturier, E.; Breton, C.; Trainer, M. G.; Szopa, C. Selection and Analytical Performances of the Dragonfly Mass Spectrometer Gas Chromatographic Columns to Support the Search for Organic Molecules of Astrobiological Interest on Titan. *Astrobiology* **2023**, *23* (2), 213–229.

(15) Barnes, J. W.; Turtle, E. P.; Trainer, M. G.; Lorenz, R. D.; MacKenzie, S. M.; Brinckerhoff, W. B.; Cable, M. L.; Ernst, C. M.; Freissinet, C.; Hand, K. P.; et al. Science Goals and Objectives for the Dragonfly Titan Rotorcraft Relocatable Lander. *Planet. Sci. J.* **2021**, *2*, No. 130.

(16) Grubisic, A.; Trainer, M. G.; Li, X.; Brinckerhoff, W. B.; van Amerom, F. H.; Danell, R. M.; Costa, J. T.; Castillo, M.; Kaplan, D.; Zacny, K. Laser Desorption Mass Spectrometry at Saturn's moon Titan. *Int. J. Mass Spectrom.* **2021**, *470*, No. 116707.

(17) Thenot, J. P.; Ruo, T. L.; Bouwsma, O. J. Formylation of secondary-amines with dimethylformamide dimethylacetal. *Anal. Lett.* **1980**, *13* (9), 759–769.

(18) Gümüç, M.; Koca, I. Enamines and Dimethylamino Imines as Building Blocks in Heterocyclic Synthesis: Reactions of DMF-DMA Reagent with Different Functional Groups. *ChemistrySelect* **2020**, *5* (40), 12377–12397, DOI: [10.1002/slct.202002205](https://doi.org/10.1002/slct.202002205).

(19) Kataoka, H.; Kijima, K.; Maruo, G. Determination of mutagenic heterocyclic amines in combustion smoke samples. *Bull. Environ. Contam. Toxicol.* **1998**, *60* (1), 60–67.

(20) Fathi, A. A.-S.; Sayed, A. S. M.; Sherif, M. S. Dimethylformamide dimethyl acetal as a building block in heterocyclic synthesis. *J. Heterocycl. Chem.* **2009**, *46*, 801–827, DOI: 10.1002/jhet.69.

(21) Freissinet, C.; Buch, A.; Sternberg, R.; Szopa, C.; Geffroy-Rodier, C.; Jelinek, C.; Stambouli, M. Search for evidence of life in space: Analysis of enantiomeric organic molecules by N,N-dimethylformamide dimethylacetal derivative dependant Gas Chromatography–Mass Spectrometry. *J. Chromatogr. A* **2010**, *1217*, 731–740.

(22) Boulesteix, D.; Buch, A.; Samson, J.; Freissinet, C.; Coscia, D.; He, Y.; Teinturier, S.; Stern, J. C.; Trainer, M. G.; Szopa, C. Dimethylformamide dimethyl acetal reagent for in situ chiral analyses of organic molecules on Titan with the Dragonfly mass spectrometer space instrument (Dragonfly mission). *J. Chromatogr. A* **2024**, *1722*, No. 464860.

(23) Moldoveanu, S. C. *Pyrolysis of Organic Molecules—Applications to Health and Environmental Issues*; Elsevier, 2009.

(24) Grubb, M. F.; Callery, P. S. Derivatization Of N-Methyl And Cyclic Amino-Acids With Dimethylformamide Dimethyl Acetal. *J. Chromatogr. A* **1989**, *469*, 191–196.

(25) Mozga, T.; Prokop, Z.; Chaloupková, R.; Damborsky, J. Chiral aliphatic hydroxy compounds in nature: A review of biological functions and practical applications. *Collect. Czech. Chem. Commun.* **2009**, *74* (7–8), 1195–1278.

(26) Boulesteix, D.; Buch, A.; Williams, A. J.; He, Y.; Freissinet, C.; Trainer, M. G.; Stern, J. C.; Szopa, C. Comparison of tetramethylammonium hydroxide (TMAH), trimethylsulfonium hydroxide (TMSH), and trimethylphenylammonium hydroxide (TMPAH) thermochemolysis for in situ space analysis of organic molecules in planetary environments. *Talanta* **2023**, *257*, No. 124283.

(27) Li, X.; van Amerom, F.; Graham, J. D.; Grubisic, A.; Francom, M. B.; Barfknecht, P. W.; Brinckerhoff, W. B.; Trainer, M. G.; Castillo, M. E. *Laser Desorption Mass Spectrometry of Cryogenic Samples on the Dragonfly Mission*, IEEE Aerospace Conference; IEEE, 2023.